Journal of the European Ceramic Society 36 (2016) 1399–1405

Contents lists available at www.sciencedirect.com

Journal of the European Ceramic Society

journal homepage: www.elsevier.com/locate/jeurceramsoc

Effects of structural characteristics on microwave dielectric properties of $MgTi_{1-x}(Mg_{1/3}B_{2/3})_xO_3$ (B = Nb, Ta)

Hyun Jin Jo, Eung Soo Kim*

Department of Materials Engineering, Kyonggi University, Suwon 443-760, Republic of Korea

ARTICLE INFO

Article history:
Received 31 August 2015
Received in revised form
14 December 2015
Accepted 22 December 2015
Available online 4 January 2016

Keywords:
$MgTiO_3$
Microwave dielectric properties
Covalency
Cation-ordering
Octahedral distortion

ABSTRACT

The dependence of the microwave dielectric properties of $MgTi_{1-x}(Mg_{1/3}B_{2/3})_xO_3$ (B = Nb, Ta, $0.03 \le x \le 0.20$) ceramics on their structural characteristics was investigated. A single phase with the ilmenite structure was confirmed through the entire range of compositions. As the $(Mg_{1/3}B_{2/3})^{4+}$ content increased at the Ti^{4+} sites, the unit-cell volume and the average octahedral distortion increased, while the tolerance factor decreased. These results could be attributed to the decrease of both quality factor (*Qf*) and temperature coefficient of resonant frequency (*TCF*) of the specimens. $MgTi_{1-x}(Mg_{1/3}B_{2/3})_xO_3$ ceramic specimens with $B = Ta^{5+}$ showed lower dielectric constant (*K*) and higher *Qf* value than those with $B = Nb^{5+}$ because of their high degree of average covalency. Although the dielectric polarizability of $(Mg_{1/3}B_{2/3})^{4+}$ was larger than that of Ti^{4+}, the *K* value of the specimens decreased linearly with $(Mg_{1/3}B_{2/3})^{4+}$ substitution because of the decrease of relative densities of the specimens.

1. Introduction

With the increasing demand for high frequency communications systems, microwave dielectric materials with a high quality factor (*Qf*) are becoming more important than ever. High *Qf* values for the enhancement of frequency selectivity, low dielectric constant (*K*) for fast signal speed, and near-zero temperature coefficient of resonant frequency (*TCF*) for improving the thermal stability of resonance are required to get better device functionality [1].

$MgTiO_3$ ceramics [2] with the ilmenite structure have received attention as high *Qf* dielectrics, along with Zn_2SiO_4 [3], Mg_2SiO_4 [4], Al_2O_3 [5], and $Mg_4Nb_2O_9$ [6]. This structure possesses two types of oxygen octahedra: one is a divalent cation (A^{2+}) octahedron (AO_6), and the other is a tetravalent cation (B^{4+}) octahedron (BO_6). Between these oxygen octahedra, face sharing is observed for the same type of oxygen octahedra, while edge sharing is observed for the different type of oxygen octahedra [2]. It has been reported that the type of sharing of the oxygen octahedra could affect the microwave dielectric properties. The crystal structures connected by edge or face sharing of oxygen octahedra showed high *Qf* values because of the improved stability of the crystal structure [7]. Based on these reports, the microwave dielectric properties are influenced by the intrinsic structural characteristics as well as by extrinsic factors such as the presence of secondary phases, density, and grain morphology [8]. Structural characteristics could be evaluated by the degree of covalency [9–11] indicating the type of bonding, the effect of cation-ordering observed by Raman spectroscopy [12], and the octahedral distortion [13] calculated by the individual bond length in oxygen octahedra using Rietveld refinement [14].

To improve the *Qf* value of $MgTiO_3$ ceramics, divalent substitute cations, such as Ni [15], Zn [16], and Co [17] for the Mg sites and tetravalent substitute cations, such as Sn [16] and Zr [18] for the Ti sites have been widely investigated. With reference to ABO_3 perovskite ceramics, the high *Qf* values can be obtained not only by the substitution of the tetravalent cations at the B-sites [19,20], but also by the isovalent substitution of combinations of aliovalent cations such as $(Li_{1/4}B_{3/4})^{4+}$ [21], $(Mg_{1/3}B_{2/3})^{4+}$ [22], and $(Al_{1/2}B_{1/2})^{4+}$ [23] (B = Nb and Ta) at the B-sites. Therefore, isovalent substitutions merit consideration for the improvement of the *Qf* of $MgTiO_3$ ceramics. According to Kuang et al. [24], the isovalent substitution of $(Mg_{1/3}Ta_{2/3})^{4+}$ in the Ti site in the ilmenite $MgTiO_3$ ceramics was attempted, but the dependence of the dielectric properties on the structural characteristics was not reported.

In this study, the effect on the microwave dielectric properties of $MgTiO_3$ ceramics resulting from isovalent substitution of $(Mg_{1/3}B_{2/3})^{4+}$ (B = Nb and Ta) at the Ti sites was investigated. Also, the dependence of the dielectric properties on the struc-

* Corresponding author.
E-mail address: eskim@kyonggi.ac.kr (E.S. Kim).

http://dx.doi.org/10.1016/j.jeurceramsoc.2015.12.033
0955-2219/

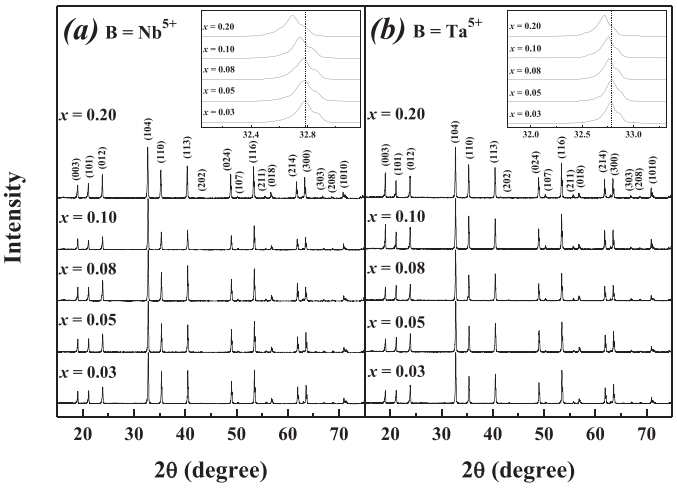

Fig. 1. X-ray diffraction patterns of (a) $MgTi_{0.95}(Mg_{1/3}Nb_{2/3})_{0.05}O_3$ and (b) $MgTi_{0.95}(Mg_{1/3}Ta_{2/3})_{0.05}O_3$ specimens sintered at 1400 °C for 4 h.

tural characteristics of $(Mg_{1/3}B_{2/3})^{4+}$ substituted $MgTiO_3$ ceramics [$MgTi_{1-x}(Mg_{1/3}B_{2/3})_xO_3$ (B = Nb, Ta) ($0.03 \le x \le 0.20$)] was studied.

2. Experimental procedures

$MgTi_{1-x}(Mg_{1/3}B_{2/3})_xO_3$ (B = Nb, Ta) ($0.03 \le x \le 0.20$) were prepared by a solid-state reaction method. High-purity oxide powders of MgO (99.9%), TiO_2 (99.9%), Nb_2O_5 (99.9%), and Ta_2O_5 (99.9%) were used as starting materials. The mixed powders were milled with ZrO_2 balls for 24 h in ethanol. The powders were calcined from 1100 to 1150 °C for 4 h and the calcined powders were milled again with ZrO_2 balls for 24 h in ethanol, and then dried. Finally, the powders were isostatically pressed into pellets under a pressure of 1500 kg/cm^2. These pellets were sintered at 1400 °C for 4 h in air.

The relative densities of the specimens were obtained from the ratio of the apparent densities measured by the Archimedes method to the true densities measured by helium pycnometer (AccuPyc 1330, Micromeritics, USA). Powder X-ray diffraction analysis (XRD) (D/Max-3C, Rigaku, Japan) was used for the phase identification. The Rietveld refinement method was employed to analyze the crystal structure on the basis of the XRD results, using the FullProf software program (WinPLOTR) [14]. The initial structure model for ilmenite compounds was taken from the study by Wechsler and Von Dreele, who used neutron powder diffraction [25]. The microstructures of the sintered specimens were observed using a scanning electron microscope (SEM) (JSM-6500F, JEOL, Japan). The average grain size was evaluated by the linear-intercept method [26]. Raman spectroscopy, to confirm the Ti-site ordering, was conducted with a Raman spectrometer (T64000, HORIBA Jobin Yvon, France) using an Ar^+ ion laser operating at 514 nm.

The dielectric constant (K) and unloaded Q of the specimens were measured by the post-resonant method developed by Hakki and Coleman [27]. The temperature coefficient of the resonant frequency (TCF) of the specimens was measured by the cavity method over a temperature range from 25 to 80 °C [28].

3. Results and discussion

3.1. Physical properties of $MgTi_{1-x}(Mg_{1/3}B_{2/3})_xO_3$ (B = Nb, Ta)

X-ray diffraction (XRD) patterns of $MgTi_{1-x}(Mg_{1/3}B_{2/3})_xO_3$ (B = Nb, Ta) ($0.03 \le x \le 0.20$) specimens sintered at 1400 °C for 4 h are shown in Fig. 1. The rhombohedral ilmenite structure was found to be present without any secondary phases throughout the entire range of both compositions with B = Nb^{5+} (Fig. 1 (a)) and Ta^{5+} (Fig. 1 (b)). With increasing $(Mg_{1/3}B_{2/3})^{4+}$ substitution, both compositions showed a shift of the XRD peaks from $2\theta = 32–33^\circ$ to lower values of 2θ, indicating the enlargement of the unit-cell volume of both compositions, as shown in the insets of Fig. 1. These results could be affected by the increase of the average Ti-site ionic radius due to the larger ionic radii of $(Mg_{1/3}B_{2/3})^{4+}$ (0.667 Å) (Mg^{2+} = 0.72 Å, Nb^{5+} and Ta^{5+} = 0.64 Å [13]), compared to that of Ti^{4+} (0.605 Å) [13] at the same coordination number of 6.

With the increase of $(Mg_{1/3}B_{2/3})^{4+}$ substitution, the apparent densities of both compositions increased in proportion to their atomic weight, as shown in Table 1. Although the relative densities of both compositions were slightly decreased by the $(Mg_{1/3}B_{2/3})^{4+}$ substitution, they still remained above 97% over the entire range of both compositions.

For microwave dielectrics, the dielectric constant (K) is affected by the theoretical dielectric polarizabilities [29] of the constituent ions as well as the relative densities [30] of the specimens. However, the K values of both compositions decreased with $(Mg_{1/3}B_{2/3})^{4+}$ substitution in spite of the larger average dielectric polarizabilities of $(Mg_{1/3}Nb_{2/3})^{4+}$ (3.09 Å^3) and $(Mg_{1/3}Ta_{2/3})^{4+}$ (3.59 Å^3) (Mg^{2+} = 1.32 Å^3, Nb^{5+} = 3.97 Å^3 and Ta^{5+} = 4.73 Å^3), compared to that of Ti^{4+} (2.93 Å^3), as shown in Table 1. Therefore, the effect of relative densities on the K value of the specimens must be taken into account. In these systems, the K values of both compositions decreased with the reduction of relative densities of the specimens.

SEM micrographs of $MgTi_{1-x}(Mg_{1/3}B_{2/3})_xO_3$ (B = Nb, Ta) ($0.03 \le x \le 0.20$) specimens sintered at 1400 °C for 4 h are shown in Fig. 3. For both compositions with B = Nb^{5+} (Fig. 2(a)–(e)) and Ta^{5+} (Fig. 2(f)–(j)), there was no remarkable change of their average grain sizes (nearly 16–17 μm) with $(Mg_{1/3}B_{2/3})^{4+}$ substitution, as shown in Table 1. This means that—in neither case—can the dielectric properties be explained by microstructural characteristics, and must, therefore, be explainable on the basis of structural characteristics.

3.2. Dependence of dielectric properties on the structural characteristics of $MgTi_{1-x}(Mg_{1/3}B_{2/3})_xO_3$ (B = Nb, Ta)

To enable the formation of a stable ilmenite structure, both the tolerance factor (t) and the electronegativity difference (Δe) of the composition should equal or exceed the values of 0.80 and 1.465, respectively [31,32]. The modified t value for the ABO_3 ilmenite structure was calculated using Eq. (1) [31]

$$t = \left(\frac{1}{3}\right)\frac{\left(\sqrt{2}+1\right)R_O + R_B}{(R_O + R_A)} + \frac{\sqrt{2}R_O}{R_O + R_B} \quad (1)$$

where R_A, R_B, and R_O are the radii of A ions, B ions, and O ions, respectively. The bonding type of constituent ions in an ABO_3 ilmenite structure can easily be calculated from the Δe value of Eq. (2) [32]

$$\Delta e = \frac{X_{A-O} + X_{B-O}}{2} \quad (2)$$

where X_{A-O} or X_{B-O} is the electronegativity difference between the A- or B-site cation and the oxygen ion, respectively. Regardless of the amount of $(Mg_{1/3}B_{2/3})^{4+}$ substitution, both compositions met the abovementioned requirements for t and Δe. Table 2 shows that the t values decreased with increasing $(Mg_{1/3}B_{2/3})^{4+}$ substitution because of the increased lattice mismatch arising from the difference of ionic radii between $(Mg_{1/3}B_{2/3})^{4+}$ and Ti^{4+}, while the Δe values increased with an increasing ratio of ionic bonding type [16]. Both results indicated that the structural stability of $MgTi_{1-x}(Mg_{1/3}B_{2/3})_xO_3$ (B = Nb, Ta) specimens decreased with the increase of $(Mg_{1/3}B_{2/3})^{4+}$ substitution; this could be expected to weaken the dielectric properties.

Table 1
Densities, theoretical dielectric polarizability, dielectric constant (K) and average grain size of $MgTi_{1-x}(Mg_{1/3}B_{2/3})_xO_3$ (B = Nb, Ta) specimens sintered at 1400 °C for 4 h.

x (mol)	Apparent density (g/cm^3)	True density (g/cm^3)	Relative density (%)	Theoretical dielectric polarizability ($Å^3$)	Dielectric constant (K)	Average grain size (μm)
$B = Nb^{5+}$						
0.03	3.911	3.981	98.2	10.285	18.2 (±0.3%)	17.05
0.05	3.921	3.993	98.2	10.288	18.0 (±0.1%)	17.20
0.08	3.935	4.017	98.0	10.293	17.9 (±0.3%)	17.34
0.10	3.945	4.048	97.4	10.296	17.8 (±0.3%)	16.46
0.20	3.995	4.088	96.7	10.311	17.4 (±0.2%)	16.70
$B = Ta^{5+}$						
0.03	3.968	4.042	98.2	10.300	18.1 (±0.1%)	16.65
0.05	4.014	4.092	98.0	10.313	18.0 (±0.2%)	17.01
0.08	4.084	4.164	98.0	10.333	17.9 (±0.2%)	17.72
0.10	4.133	4.241	97.5	10.346	17.5 (±0.3%)	17.40
0.20	4.401	4.580	96.0	10.413	17.1 (±0.3%)	17.54

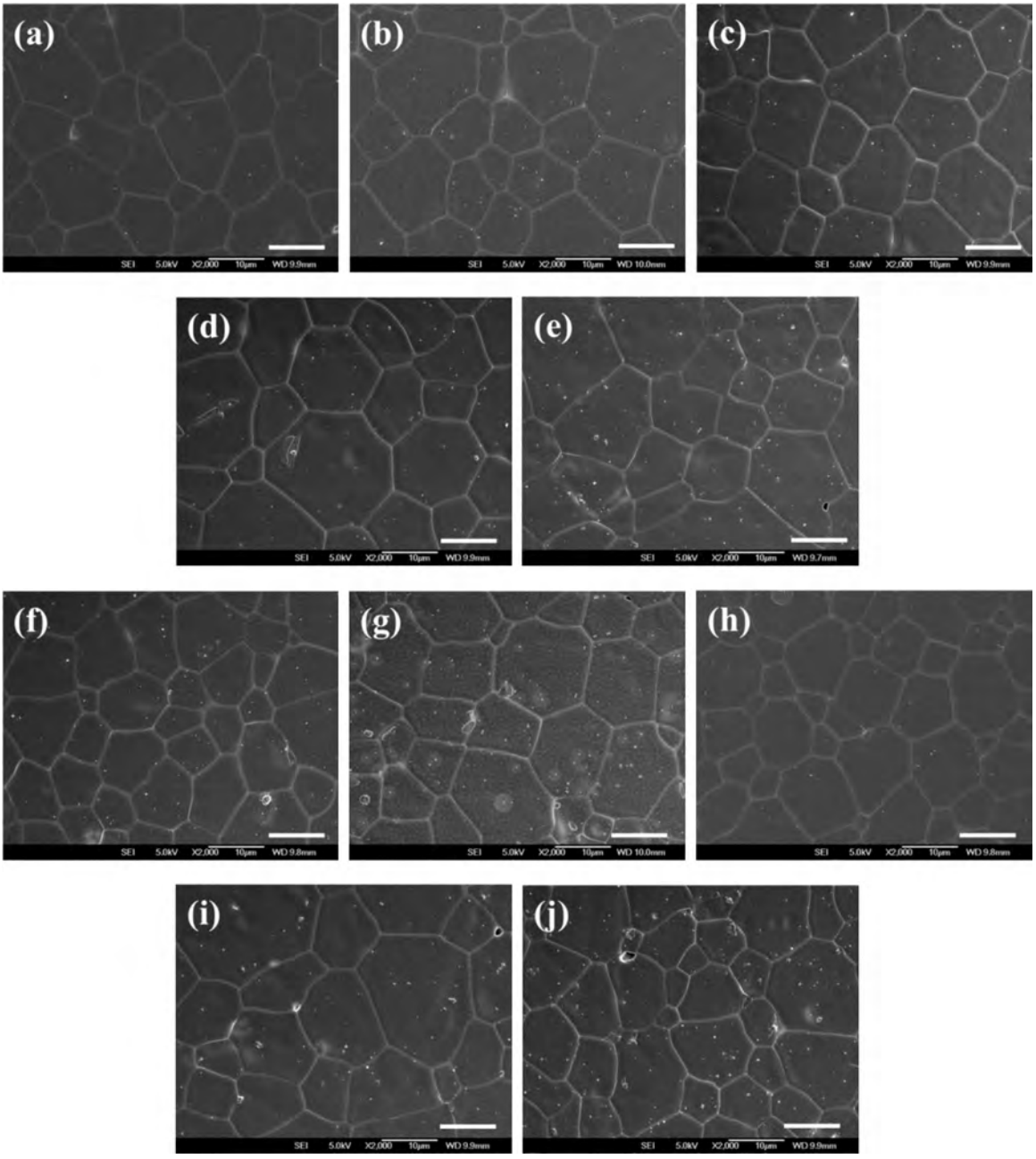

Fig. 2. SEM micrographs of $MgTi_{1-x}(Mg_{1/3}Nb_{2/3})_xO_3$ specimens sintered at 1400 °C for 4 h: (a) $x = 0.03$, (b) $x = 0.05$, (c) $x = 0.08$, (d) $x = 0.10$, (e) $x = 0.20$ and $MgTi_{1-x}(Mg_{1/3}Ta_{2/3})_xO_3$ specimens sintered at 1400 °C for 4 h: (f) $x = 0.03$, (g) $x = 0.05$, (h) $x = 0.08$, (i) $x = 0.10$, (j) $x = 0.20$ (bar = 10 μm).

Table 2
Refined structural parameters of $MgTi_{1-x}(Mg_{1/3}B_{2/3})_xO_3$ (B = Nb, Ta) specimens sintered at 1400 °C for 4 h.

x (mol)	*R*-factor		Lattice parameter (Å)		$V_{unit\text{-}cell}$ (Å^3)	Tolerance factor (t)	Electro negativity difference (Δe)
	R_{Bragg}	GoF	*a*-axis	*c*-axis			
B = Nb^{5+}							
0.03	6.04	2.3	5.0575	13.9018	307.94	0.9526	2.016
0.05	4.46	2.0	5.0593	13.9093	308.33	0.9526	2.016
0.08	6.38	2.7	5.0633	13.9123	308.88	0.9526	2.016
0.10	6.80	2.8	5.0655	13.9141	309.19	0.9525	2.017
0.20	5.43	2.4	5.0759	13.9320	310.86	0.9525	2.019
B = Ta^{5+}							
0.03	4.84	2.2	5.0572	13.9020	307.91	0.9526	2.017
0.05	4.71	2.4	5.0594	13.9045	308.24	0.9526	2.018
0.08	5.17	2.2	5.0626	13.9096	308.74	0.9526	2.019
0.10	5.39	2.5	5.0640	13.9143	309.02	0.9525	2.020
0.20	5.30	2.8	5.0659	13.9153	309.27	0.9525	2.025

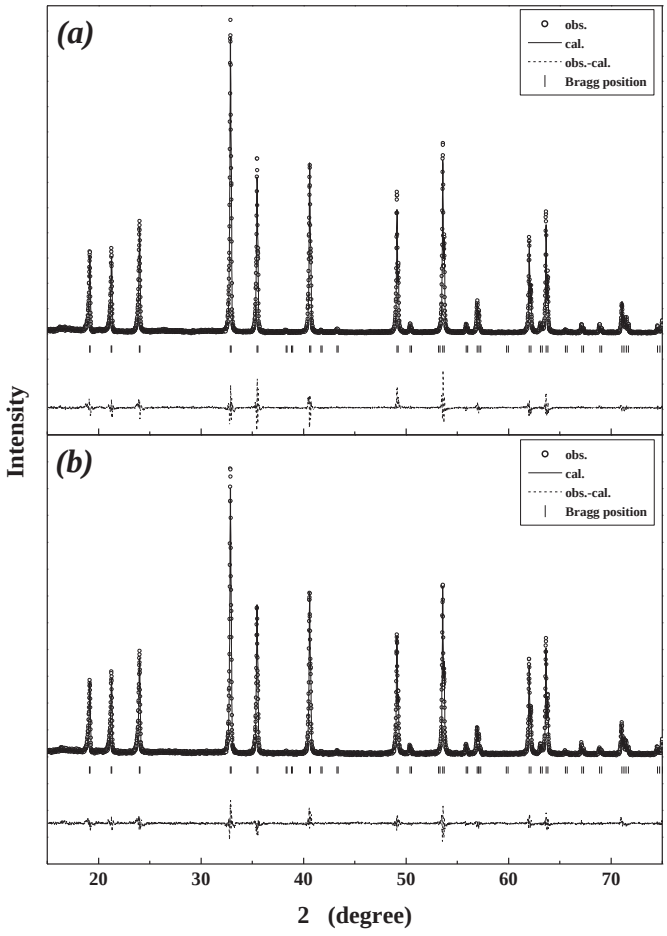

Fig. 3. Rietveld refinement patterns of (a) $MgTi_{0.95}(Mg_{1/3}Nb_{2/3})_{0.05}O_3$ and (b) $MgTi_{0.95}(Mg_{1/3}Ta_{2/3})_{0.05}O_3$ specimens sintered at 1400 °C for 4 h.

Fig. 3 shows the Rietveld refinement patterns of $MgTi_{1-x}(Mg_{1/3}B_{2/3})_xO_3$ (B = Nb, Ta) ($0.03 \le x \le 0.20$) specimens; the corresponding structural parameters are presented in Table 2. The data points in Fig. 3 are the observed intensities, the overlying solid lines are calculated intensities, and the bottom line corresponds to the difference between the observed and calculated intensities; these refined results showed good reliabilities. Lattice parameters and unit-cell volumes for both compositions were increased by $(Mg_{1/3}B_{2/3})^{4+}$ substitution. However, the specimens with B = Ta^{5+} showed smaller lattice parameters and unit-cell volumes than those with B = Nb^{5+} despite the fact that Nb^{5+} and Ta^{5+} have the same atomic radii (0.64 Å) [13] at a coordination number of 6.

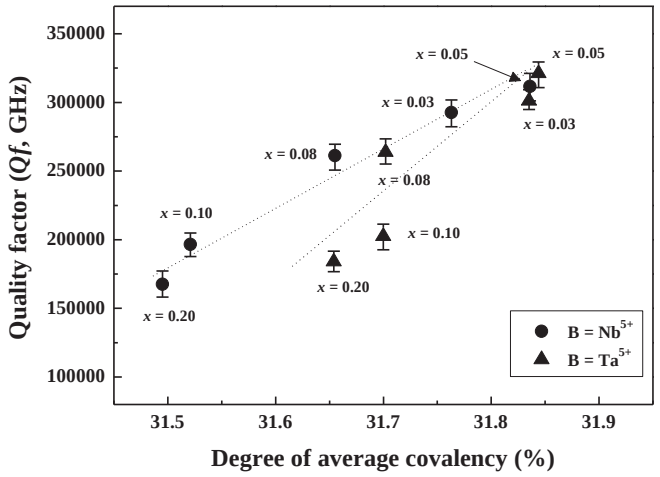

Fig. 4. Dependence of quality factor (*Qf*) on the degree of average covalency of $MgTi_{1-x}(Mg_{1/3}B_{2/3})_xO_3$ (B = Nb, Ta) specimens sintered at 1400 °C for 4 h.

Similar results have been previously reported for dielectrics with the rutile structure [33]. This difference might result from the effect of bond characteristics for both compositions.

To evaluate the bond characteristics of $MgTi_{1-x}(Mg_{1/3}B_{2/3})_xO_3$ (B = Nb, Ta) ($0.03 \le x \le 0.20$) specimens, the degree of covalency was calculated from the relationship between bond strength (*s*) and covalency (f_c) using [9–11],

$$s = \left(\frac{R_{avg}}{R_1}\right)^{-N}, \quad (3)$$

$$f_c = as^M, \quad (4)$$

$$\text{and the degree of covalency}\,(\%) = \frac{f_c}{s} \times 100 \quad (5)$$

where $R_{avg.}$ is the average bond length between the cation and oxygen ion, while R_1 and *N* are empirical constants that depend on the cation site and are different for each octahedral cation – oxygen ion pair [10]. Moreover, *a* and *M* are empirical constants that depend on the number of electrons [9]. Fig. 4 shows the dependence of *Qf* on the degree of average covalency for both the Nb^{5+} and the Ta^{5+} compositions. As the degree of average covalency increased, the *Qf* values of both compositions increased linearly. Moreover, the specimens with B = Ta^{5+} indicated a higher degree of average covalency and higher *Qf* values than those with B = Nb^{5+}. It has been reported that covalent bonds between the cation and the oxygen ion in oxygen octahedra could be stronger than ionic bonds [16]. The enhanced bond strength between the cation and the oxygen ion could lead to a decrease of lattice parameters and unit-cell volume, as well as an increase in the stability of the crystal structure.

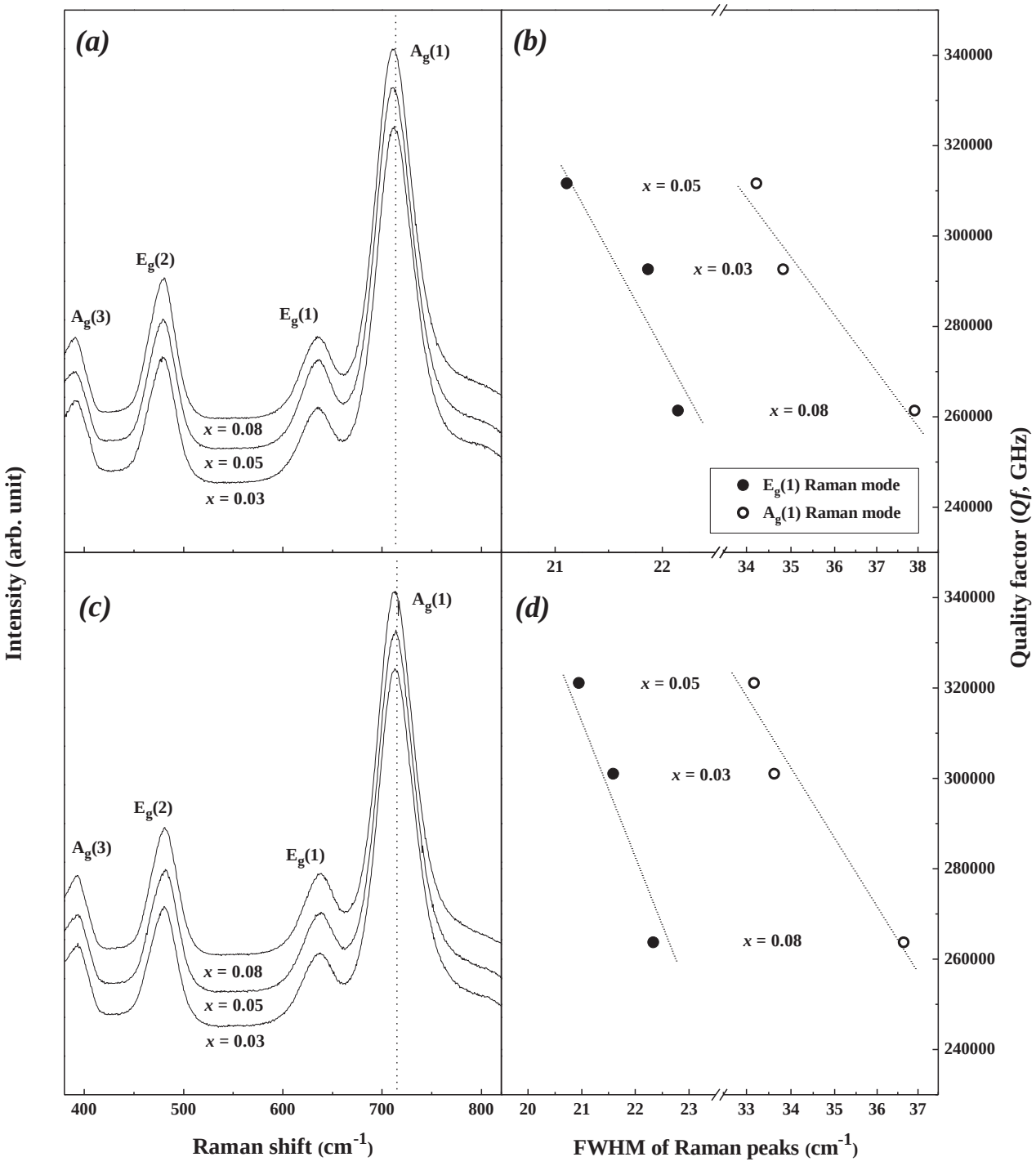

Fig. 5. Shifting of Raman peaks and relationships between FWHM values of $A_g(1)$ and $E_g(1)$ Raman modes and quality factors (Qf) of $MgTi_{0.95}(Mg_{1/3}Nb_{2/3})_{0.05}O_3$ ($0.03 \le x \le 0.08$) ((a), (c)) and $MgTi_{0.95}(Mg_{1/3}Ta_{2/3})_{0.05}O_3$ specimens ($0.03 \le x \le 0.08$) ((b), (d)) sintered at 1400 °C for 4 h.

It was the reason for the high Qf value of the specimens with B = Ta^{5+}. However, the Qf values did not show a linear dependence on the value of x for either of the two compositions, with the amount of $(Mg_{1/3}B_{2/3})^{4+}$ substitution due to $x = 0.05$ for both compositions. The Qf values increased from $x = 0.03$ to $x = 0.05$, and then decreased gradually for further increases in x. These phenomena were related to the effects of cation-ordering in the crystal structure, which led to the improved Qf values, and generated near 0.05 mol substitution for dielectric materials [34].

Fig. 5 shows the Raman spectra of $MgTi_{1-x}(Mg_{1/3}B_{2/3})_xO_3$ (B = Nb, Ta) ($0.03 \le x \le 0.08$) specimens sintered at 1400 °C for 4 h. It is well-known that Raman spectroscopy is a practical tool for confirming the degree of Ti-site ordering. For Raman spectroscopy analysis, both the shift of the Raman peaks and the full width at half maximum (FWHM) values are useful indicators of the structural characteristics. Among Raman modes in the ilmenite $MgTiO_3$ system, the peak at about 711–714 cm^{-1} is the $A_g(1)$ Raman mode and the peak at about 631–635 cm^{-1} is the $E_g(1)$ mode. Both Raman modes indicate Ti— O bond stretching [16,35]. With increasing

Table 3
Raman spectroscopic data of $MgTi_{1-x}(Mg_{1/3}B_{2/3})_xO_3$ (B = Nb, Ta) ($0.03 \le x \le 0.08$) specimens sintered at 1400 °C for 4 h.

x (mol)	FWHM of Raman peak (cm^{-1})		Raman shift (cm^{-1})	
	$A_g(1)$	$E_g(1)$	$A_g(1)$	$E_g(1)$
$B = Nb^{5+}$				
0.03	34.82	21.87	711.8	634.9
0.05	34.23	21.11	711.7	632.4
0.08	37.92	22.15	711.2	631.8
$B = Ta^{5+}$				
0.03	33.62	21.59	713.6	635.9
0.05	33.17	20.95	713.3	634.0
0.08	36.65	22.34	712.6	633.6

$(Mg_{1/3}B_{2/3})^{4+}$ substitution, the Raman peaks moved to lower frequencies in accordance with an increase of the atomic weight of the cation [36] that is located at the center of the oxygen octahedron (Fig. 5(a), (c)). Also, the peaks of the specimens with $B = Ta^{5+}$ were located at higher frequencies than those with $B = Nb^{5+}$, indicating higher bond strength between the Ti^{4+} ion and the oxygen ion [37], as shown in Table 3. These results agreed well with not only a high degree of average covalency, but also with the small K values for the specimens with $B = Ta^{5+}$. The increase of the bond strength between the cation and oxygen ion in the oxygen octahedron created more rigid octahedra, which could decrease the effect of rattling of the cation in the oxygen octahedron, and consequently decrease the K value [37]. For $x = 0.05$, in the case of $MgTi_{1-x}(Mg_{1/3}B_{2/3})_xO_3$ (B = Nb, Ta) ($0.03 \le x \le 0.08$) specimens, the highest Qf values were obtained with the narrowest FWHM values of Raman peaks (Fig. 5(b), (d)). Generally, the well-ordered structures were correlated with narrow FWHM values of the Raman peaks [12,37]. In view of the fact that the specimens with $B = Ta^{5+}$ showed narrower FWHM values than those with $B = Nb^{5+}$, it also indicated a more ordered structure in the case of the specimens with $B = Ta^{5+}$.

With increasing $(Mg_{1/3}B_{2/3})^{4+}$ substitution in $MgTi_{1-x}(Mg_{1/3}B_{2/3})_xO_3$ (B = Nb, Ta) ($0.03 \le x \le 0.20$) specimens, the individual bond lengths of the oxygen octahedra in the ilmenite structure could be distorted. According to Shannon, the distortion of the oxygen octahedra can be calculated by Eq. (6) [13]

$$\Delta = \frac{1}{6} \times \Sigma \frac{(R_i - \bar{R})}{\bar{R}} \quad (6)$$

where R_i is an individual bond length, and $\bar{R}$ is the average bond length in oxygen octahedra. Fig. 6 shows the inverse relationship between TCF values and the average octahedral distortion ($\Delta_{avg.}$) for both compositions. The TCF value of each composition decreased with the increase of $(Mg_{1/3}B_{2/3})^{4+}$ substitution along with increasing $\Delta_{avg.}$ values. The TCF of the ilmenite structure was affected by the octahedral distortion because the increase of thermal energy with temperature is supposed to be absorbed completely in recovering the octahedral distortion rather than in restoring the direct dependence of the polarizability on temperature, which led to the decrease of the TCF value [38]. The specimens with $B = Ta^{5+}$ showed slightly lower TCF value to negative than those with $B = Nb^{5+}$. These results were affected by the higher $\Delta_{avg.}$ value of the specimens with $B = Ta^{5+}$, generated from their high bond strength.

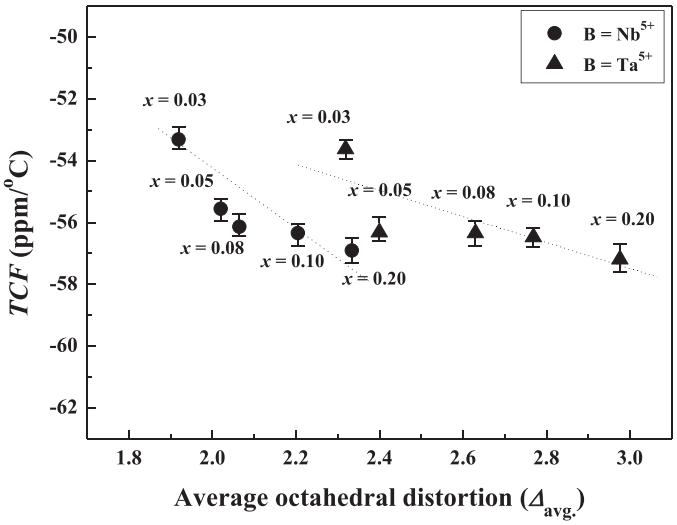

Fig. 6. Relationships between TCF value and average octahedral distortion of $MgTi_{1-x}(Mg_{1/3}B_{2/3})_xO_3$ (B = Nb, Ta) specimens sintered at 1400 °C for 4 h.

4. Conclusions

The microwave dielectric properties of $MgTi_{1-x}(Mg_{1/3}B_{2/3})_xO_3$ (B = Nb, Ta) ($0.03 \le x \le 0.20$) were investigated, based on their structural characteristics. Complete solid solutions with rhombohedral ilmenite structures were obtained through the entire range of compositions with both Nb and Ta. The specimens of $MgTi_{1-x}(Mg_{1/3}B_{2/3})_xO_3$ with $B = Ta^{5+}$ showed higher covalent bond characteristics than those with $B = Nb^{5+}$, which was confirmed by Raman spectroscopy analysis, and could result in both low dielectric constant (K) and high quality factor (Qf) for the specimens with $B = Ta^{5+}$. The K value decreased slightly with the reduction of relative densities, and the temperature coefficient of the resonant frequency (TCF) was also decreased by increasing the average octahedral distortion because of the difference of average ionic radii between Ti^{4+} (0.605 Å) and $(Mg_{1/3}B_{2/3})^{4+}$ (0.667 Å). The Qf value of the specimens depended strongly on the degree of average covalency. For the specimens with $B = Nb^{5+}$ and Ta^{5+}, the highest Qf values were observed at $x = 0.05$ because of the improved cation-ordering effect, which was confirmed by the fact that these samples also had smallest full width at half maximum (FWHM) values of their Raman peaks.

References

[1] R.J. Cava, Dielectric materials for applications in microwave communications, J. Mater. Chem. 11 (2001) 54–62.
[2] J.H. Sohn, Y. Inaguma, S.O. Yoon, M. Itoh, T. Nakamura, S.J. Yoon, H.J. Kim, Microwave dielectric characteristics of ilmenite-type titanates with high Q values, Jpn. J. Appl. Phys. 33 (1994) 5466–5470.
[3] Y. Guo, H. Ohsato, K.I. Kakimoto, Characterization and dielectric behavior of willemite and TiO_2-doped willemite ceracmis at millimeter-wave frequency, J. Eur. Ceram. Soc. 26 (2006) 1827–1830.
[4] T. Tsunooka, T. Sugiyama, H. Ohsato, K. Kakimoto, M. Andou, Y. Higashida, H. Sugihara, Development of forsterite with high Q and zero temperature coefficient τ_f for millimeterwave dielectric ceramics, Key Eng. Mater. 269 (2004) 199–202.
[5] H. Ohsato, T. Tsunooka, M. Ando, Y. Ohishi, Y. Miyauchi, K. Kakimoto, Millimeter-wave dielectric ceramics of alumina and forsterite with high quality factor and low dielectric constant, J. Korean Ceram. Soc. 40 (2003) 350–353.

[6] A. Kan, H. Ogawa, A. Yokoi, Y. Nakamura, Crystal structural refinement of corundum-structured $A_4M_2O_9$(A = Co and Mg, M = Nb and Ta) microwave dielectric ceramics by high-temperature X-ray powder diffraction, J. Eur. Ceram. Soc. 27 (2007) 2977–2981.
[7] E.S. Kim, C.J. Jeon, Dependence of microwave dielectric properties on structural characteristics of ilmenite, tri-rutile and wolframite ceramics, J. Adv. Dielectr. 1 (2011) 127–134.
[8] Q. Liao, L. Li, P. Zhang, L. Cao, Y. Han, Correlation of crystal structure and microwave dielectric properties for $Zn(Ti_{1-x}Sn_x)Nb_2O_8$ ceramics, Mater. Sci. Eng. B 176 (2011) 41–44.
[9] I.D. Brown, R.D. Shannon, Empirical bond-strength-bond-length curves for oxides, Acta Crystallogr. A 29 (1973) 266–282.
[10] I.D. Brown, K.K. Wu, Empirical parameters for calculating cation-oxygen bond valences, Acta Crystallogr. B 32 (1976) 1957–1959.
[11] A. Kan, H. Ogawa, H. Ohsato, Synthesis and crystal structure-microwave dielectric property relations in Sn-substituted $Ca_3(Zr_{1-x}Sn_x)Si_2O_9$ solid solutions with cuspidine structure, Jpn. J. Appl. Phys. 46 (2007) 7108–7111.
[12] E.S. Kim, S.N. Seo, Microwave dielectric properties of $(Zn_{1/3}Ta_{2/3})_{0.5}(Ti_{1-x}Sn_x)_{0.5}O_2$ ceramics, J. Ceram. Soc. Jpn. 116 (2008) 619–623.
[13] R.D. Shannon, Revised effective ionic radii and systematic studies of interatomic distances in halides and chalcogenides, Acta Crystallogr. A 32 (1976) 751–767.
[14] T. Roisnel, J.R. Carvajal WinPLOTR, a window tool for powder diffraction pattern analysis, Mater. Sci. Forum 378-381 (2001) 118–123.
[15] C.H. Shen, C.L. Huang, Microwave dielectric properties of $(Mg_{0.95}Ni_{0.05})TiO_3$-$SrTiO_3$ ceramics with a near-zero temperature coefficient of resonant frequency, Int. J. Appl. Ceram. Technol. 7 (2010) 207–216.
[16] H.J. Jo, J.S. Kim, E.S. Kim, Microwave dielectric properties of $MgTiO_3$-based ceramics, Ceram. Int. 41 (2015) S530–S536.
[17] L. Li, X. Ding, Q. Liao, Reaction-sintering method for ultra-low loss $(Mg_{0.95}Co_{0.05})TiO_3$ ceramics, J. Alloy Compd. 509 (2011) 7271–7276.
[18] C.F. Tseng, Microwave dielectric properties of a new ultra low loss perovskite ceramics, J. Am. Ceram. Soc. 91 (2008) 4125–4128.
[19] I.A. Souza, L.S. Cavalcante, J.C. Sczancoski, F. Moura, C.O. Paiva-Santos, J.A. Varela, A.Z. Simoes, E. Longo, Structural and dielectric properties of $Ba_{0.5}Sr_{0.5}(Sn_xTi_{1-x})O_3$ ceramics obtained by the soft chemical method, J. Alloy Compd. 477 (2009) 877–882.
[20] V. Sivasubramanian, V.R.K. Murthy, B. Viswanathan, Microwave dielectric properties of certain simple alkaline earth perovskite compounds as a function of tolerance factor, Jpn. J. Appl. Phys. 36 (1997) 194–197.
[21] S.O. Yoon, D.M. Kim, S.H. Shim, J.K. Park, K.S. Kang, Microwave dielectric properties of $Ca(Li_{1/4}Nb_{3/4})O_3$-$CaTiO_3$ ceramic systems, J. Eur. Ceram. Soc. 26 (2006) 2023–2026.
[22] F. Zhao, Z. Yue, Y. Zhang, Z. Gui, L. Li, Microstructure and microwave dielectric properties of $Ca[Ti_{1-x}(Mg_{1/3}Nb_{2/3})_x]O_3$ ceramics, J. Eur. Ceram. Soc. 25 (2005) 3347–3352.
[23] S. Kucheiko, D.H. Yeo, J.W. Choi, S.J. Yoon, H.J. Kim, Microwave dielectric properties of $CaTiO_3$-$CaAl_{1/2}Nb_{1/2}O_3$ ceramics doped with Li_3NbO_4, J. Am. Ceram. Soc. 85 (2002) 1327–1329.
[24] X.J. Kuang, H.T. Xia, F.H. Liao, C.H. Wang, L. Li, X.P. Jing, Z.X. Tang, Doping effects of Ta on conductivity and microwave dielectric loss of $MgTiO_3$ ceramics, J. Am. Ceram. Soc. 90 (2007) 3142–3147.
[25] B.A. Wechsler, R.B. Von Dreele, Structure refinements of Mg_2TiO_4, $MgTiO_3$ and $MgTi_2O_5$ by time-of-flight neutron powder diffraction, Acta Crystallogr. B 45 (1989) 542–549.
[26] Annual Book of ASTM Standards, Designation E: 112-82 (Easton, MD, 1992).
[27] B.W. Hakki, P.D. Coleman, A dielectric resonator method of measuring inductive capacities in the millimeter range, Microw. Theory Tech. 8 (1960) 402–410.
[28] T. Nishikawa, K. Wakino, H. Tamura, H. Tanaka, Y. Ishikawa, Precise measurement method for temperature coefficient of microwave dielectric resonator materials, Microw. Symp. Dig. 87 (1987) 277–280.
[29] R.D. Shannon, Dielectric polarizabilities of ions in oxides and fluorides, J. Appl. Phys. 73 (1993) 348–366.
[30] K.H. Yoon, E.S. Kim, J.S. Jeon, Understanding the microwave dielectric properties of $(Pb_{0.45}Ca_{0.55})[Fe_{0.5}(Nb_{1-x}Ta_x)_{0.5}]O_3$ ceramics via the bond valence, J. Eur. Ceram. Soc. 23 (2003) 2391–2396.
[31] X.C. Liu, R. Hong, C. Tian, Tolerance factor and the stability discussion of ABO_3-type ilmenite, J. Mater. Sci. Mater. Electron. 20 (2009) 323–327.
[32] L. Pauling, The nature of the chemical bond. IV. The energy of single bonds and the relative electronegativity of atoms, J. Am. Ceram. Soc. 54 (1932) 3570–3582.
[33] E.S. Kim, D.H. Kang, Relationships between crystal structure and microwave dielectric properties of $(Zn_{1/3}B_{2/3}{}^{5+})_xTi_{1-x}O_2$ (B^{5+} = Nb, Ta) ceramics, Ceram. Int. 34 (2008) 883–888.
[34] M.A. Akbas, P.K. Davies, Ordering-induced microstructures and microwave dielectric properties of the $Ba(Mg_{1/3}Nb_{2/3})O_3$-$BaZrO_3$ system, J. Am. Ceram. Soc. 81 (1998) 670–676.
[35] X. Wu, S. Qin, L. Dubrovinsky, Structural characterization of the $FeTiO_3$-$MnTiO_3$ solid solution, J. Solid State Chem. 183 (2010) 2483–2489.
[36] D.J. Kim, J.W. Jang, H.L. Lee, Effect of tetravalent dopants on raman spectra of tetragonal zirconia, J, Am, Ceram, Soc 80 (1997) 1453–1461.
[37] C.T. Chia, Y.C. Chen, H.F. Cheng, I.N. Lin, Correlation of microwave dielectric properties and normal vibration modes of $xBa(Mg_{1/3}Ta_{2/3})O_3$-$(1-x)Ba(Mg_{1/3}Nb_{2/3})O_3$ ceramics: I Raman spectroscopy, J. Appl. Phys. 94 (2003) 3360–3364.
[38] E.S. Kim, K.H. Yoon, Microwave dielectric properties of $(1-x)CaTiO_3$-$xLi_{1/2}Sm_{1/2}TiO_3$ ceramics, J. Eur. Ceram. Soc. 23 (2003) 2397–2401.